Electronic Supplementary Material (ESI) for Sustainable Energy & Fuels.

Supplementary Information

Photocatalytic CO_2 Reduction to Methanol Integrated with the Oxidative Coupling of Thiols to S-X (X=S, C) bond formation over $Fe_3O_4/BiVO_4$ Composite

Nitish Saini[a,b], Sandhya Saini[a,b], Santanu Majumder,[c]*Kyra Sedransk Campbell,[d] Suman L Jain[a]*

[a]*Chemical & Material Sciences Division, CSIR-Indian Institute of Petroleum, Haridwar Road, Mohkampur, Dehradun-248005, India*
[b]*Academy of Scientific and Innovative Research, Ghaziabad- 201002, India*
[c]*Faculty of Science and Technology, Bournemouth University, Talbot Campus, Fern Barrow, Poole, BH12 5BB, UK*
[d]Department of Chemical and Biological Engineering, University of Sheffield, Sheffield, S1 3JD, UK
**Email: suman@iip.res.in; smajumder@bournemouth.ac.uk*

Table of contents: **Page No**

TG-DTA of the photocatalyst

The thermal stability of the materials i.e., Fe_3O_4 and FBV-2 was determined by using thermogravimetric and derivative thermogravimetric (TGA/DTG) analysis in the temperature range 30 °C to 800 °C under N_2 environment (Figure 1). In Fe_3O_4, the first weight loss (~6 wt%) below 200 °C is observed due to the evaporation of moisture or other volatile organic moieties. The second weight loss (~10 wt%) at temperature 463 °C is attributed to the phase transition from Fe_3O_4 to thermodynamically stable FeO state.[1] After that the material remains stable upto 800 °C. Similarly, in FBV-2, the first weight loss below 200 °C is attributed to the evaporation of moisture or volatile organic moieties. The second weight loss at 425 °C is related to the Fe-O formation from $Fe_3O_4/BiVO_4$. The third weight loss at 625 °C is due to the decomposition of the constituted components of photocatalyst (FBV-2) into their oxide forms. After that the material remains stable upto 800 °C.

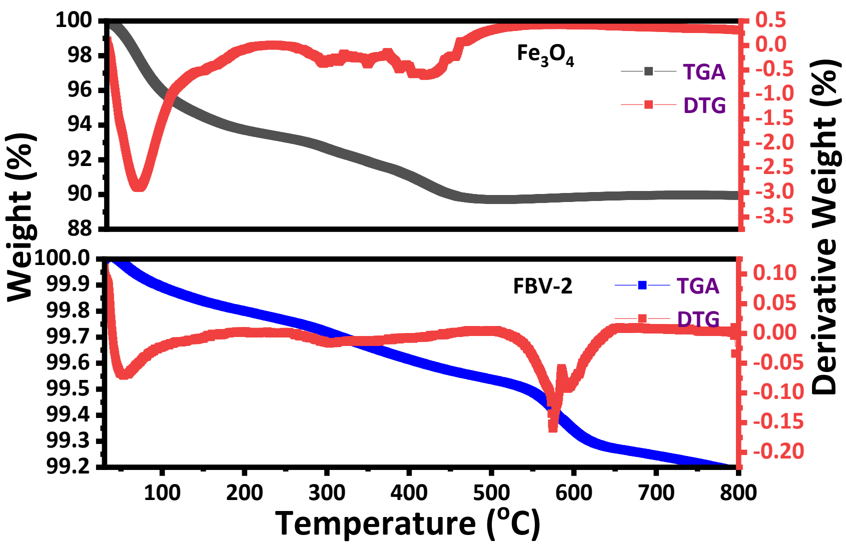

Figure S1: TG/DTA of photocatalyst Fe3O4 and FBV-2

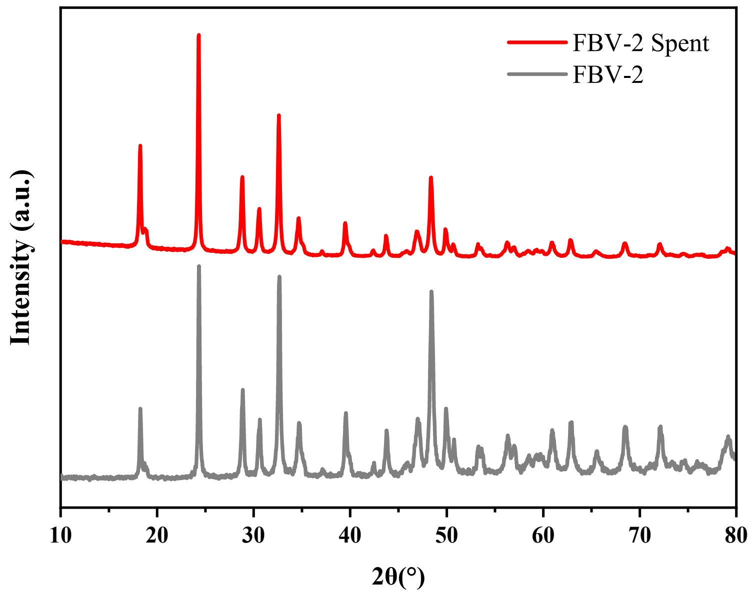

Figure S2: XRD of Fresh and spent FBV-2 for comparison

GC-MS of the products (disulfides)

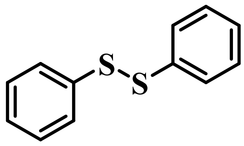

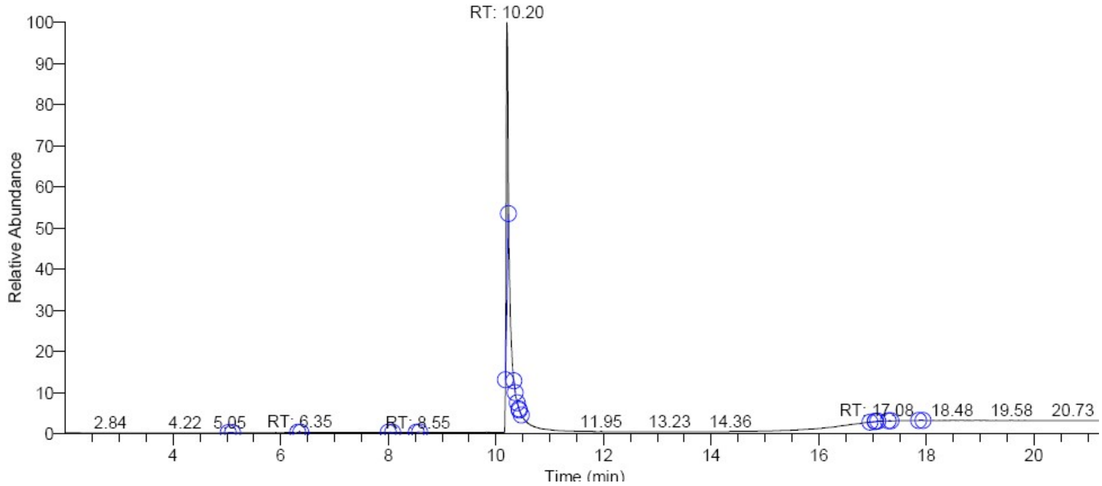

Figure S3. GC Spectra of 1,2-diphenyldisulfane

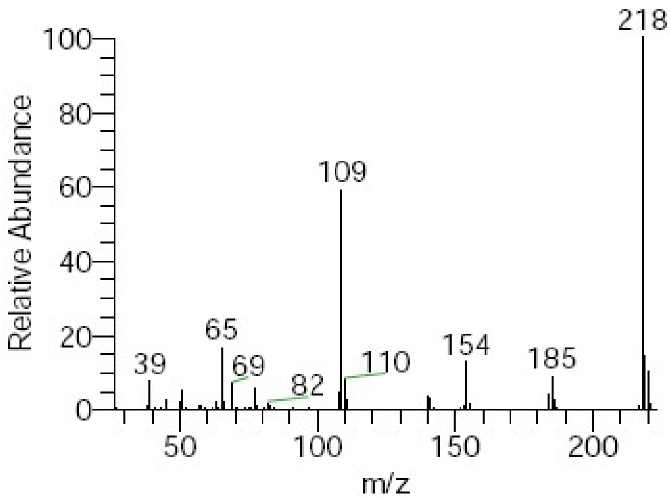

Figure S4. Mass Spectra of 1,2-diphenyldisulfane

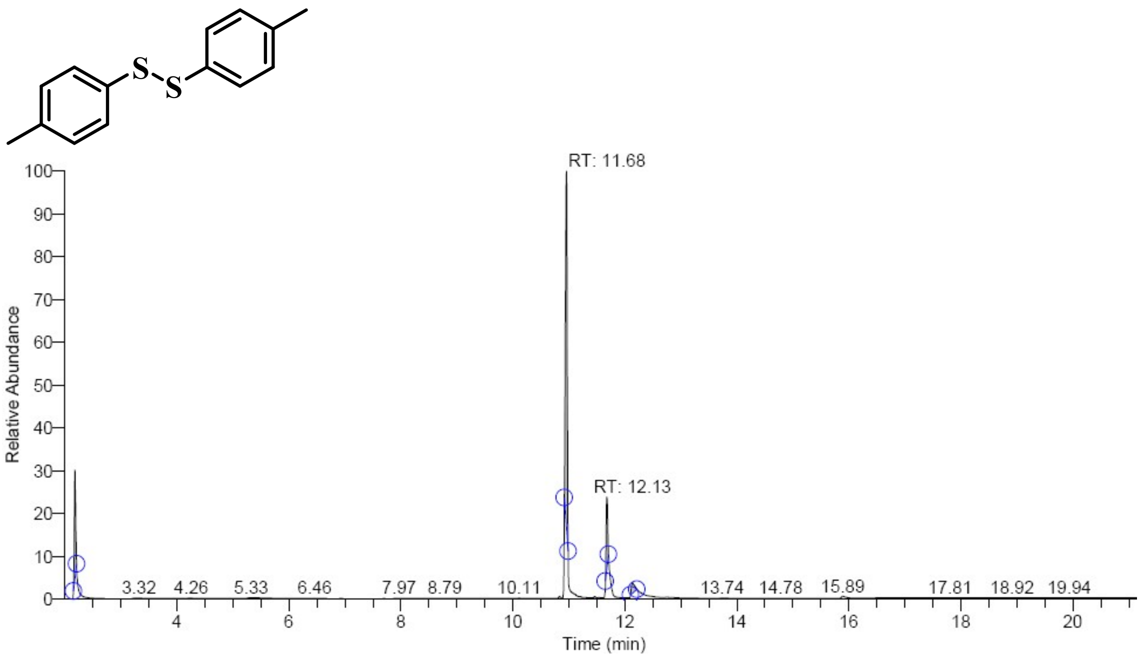

Figure S5.GC Spectra of 1,2-di-p-tolyldisulfane

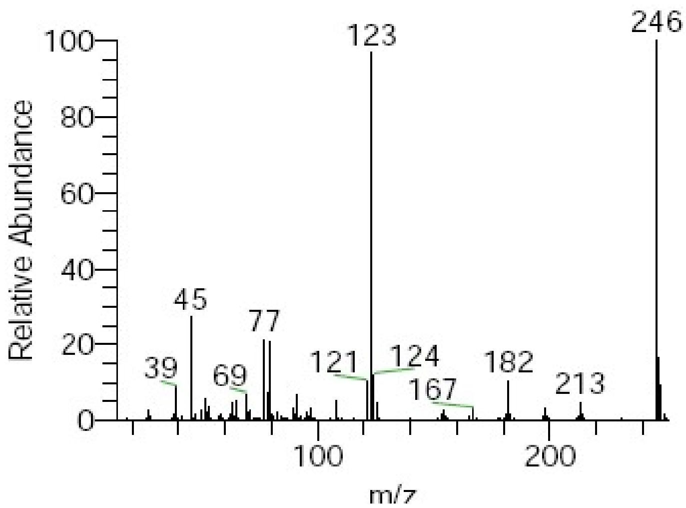

Figure S6. Mass Spectra of 1,2-di-p-tolyldisulfane

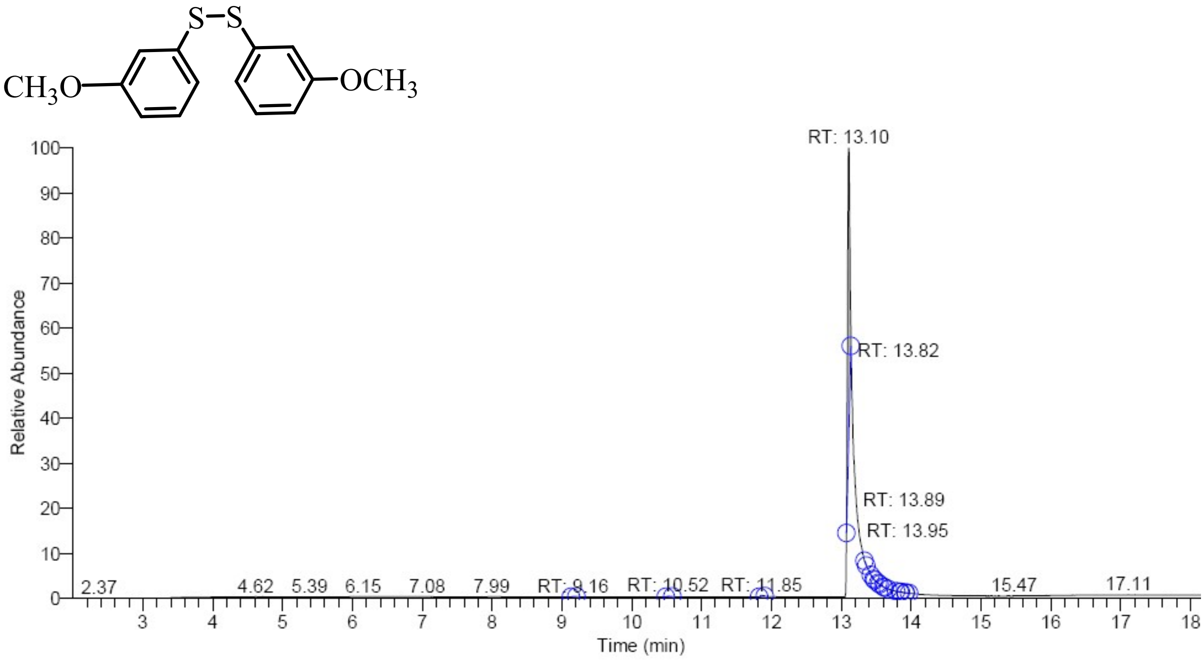

Figure S7.GC Spectra of 1,2-bis(3-methoxyphenyl) disulfane

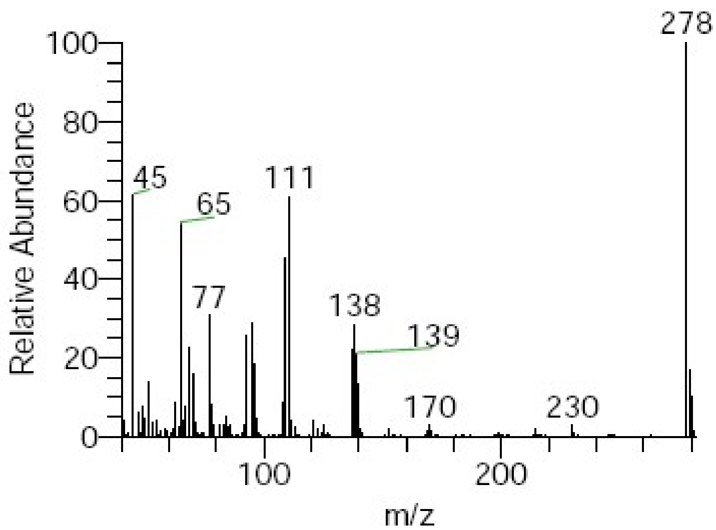

Figure S8. Mass Spectra of 1,2-bis(3-methoxyphenyl) disulfane

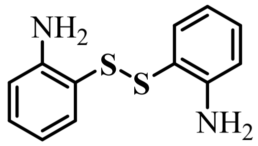

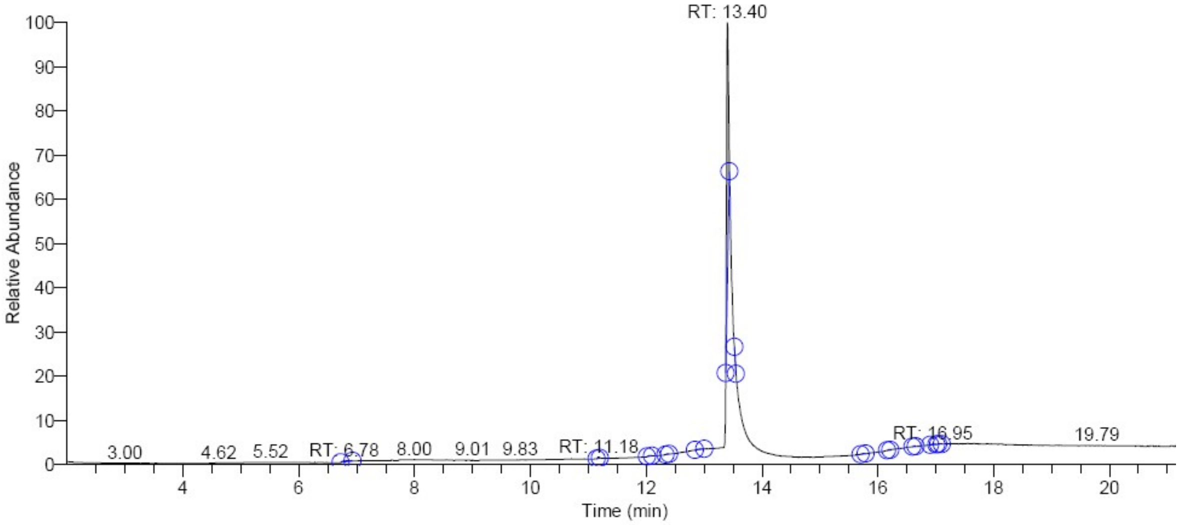

Figure S9.GC Spectra of 2,2'-disulfanediyldianiline

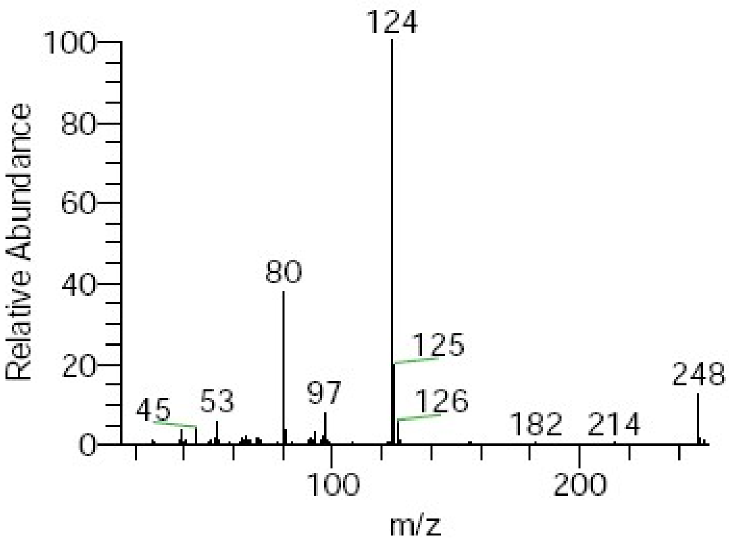

Figure S10. Mass Spectra of 2,2'-disulfanediyldianiline

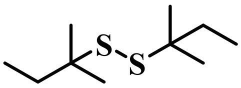

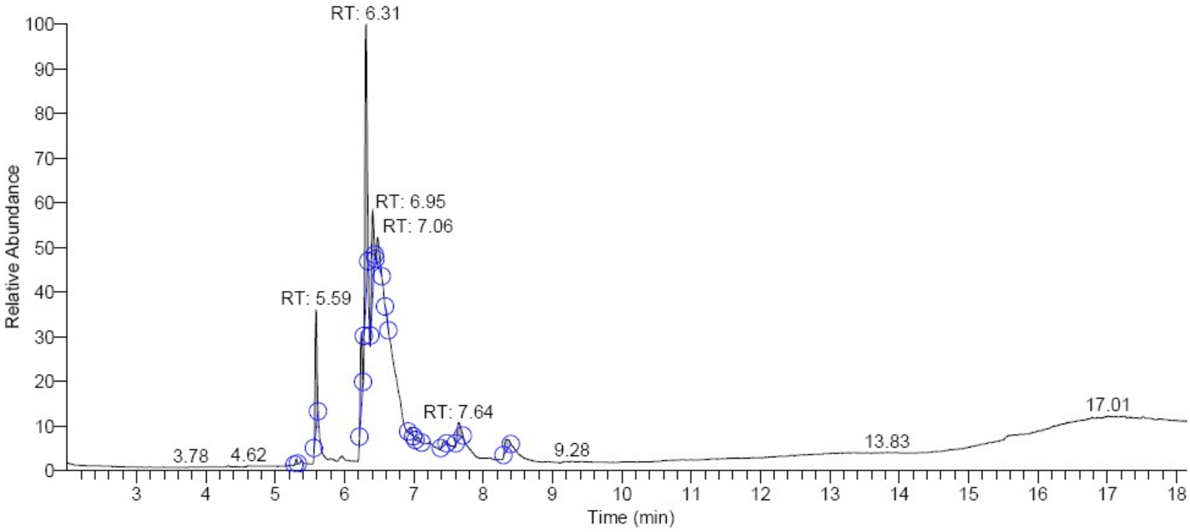

Figure S11.GC Spectra of 1,2-di-tert-pentyldisulfane

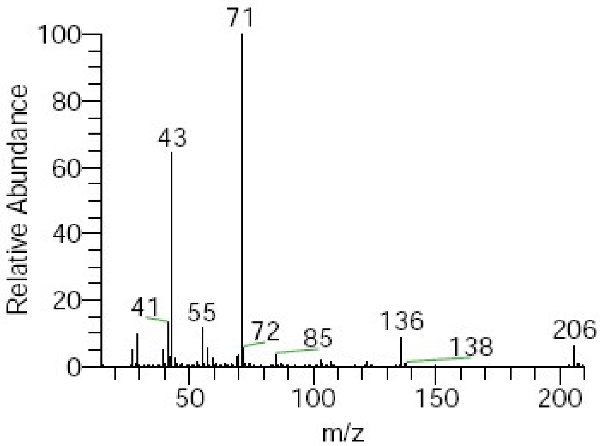

Figure S12. Mass Spectra of 1,2-di-tert-pentyldisulfane

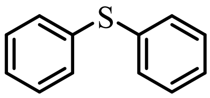

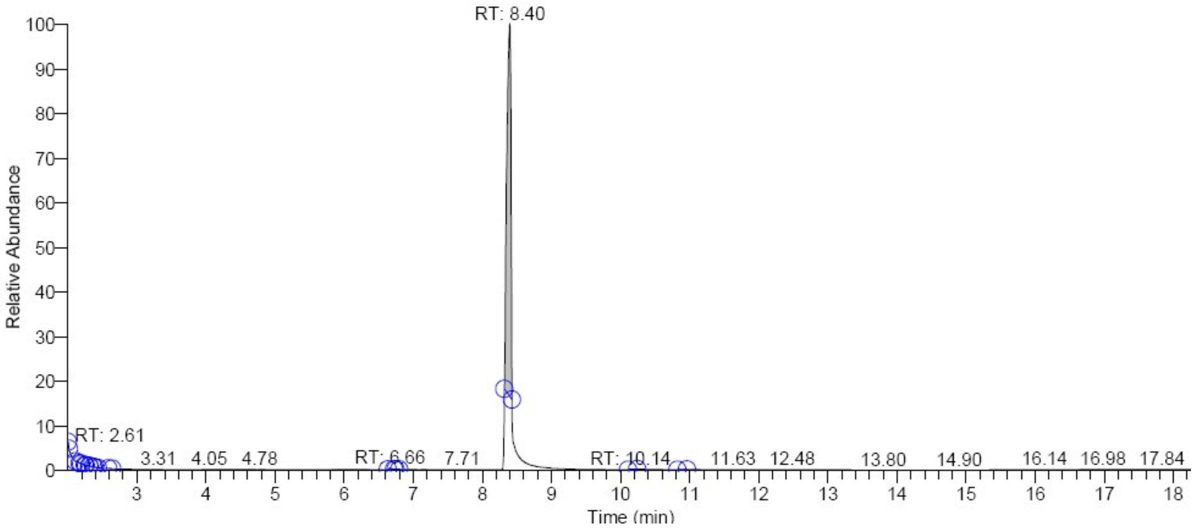

Figure S13.GC Spectra of diphenylsulfane

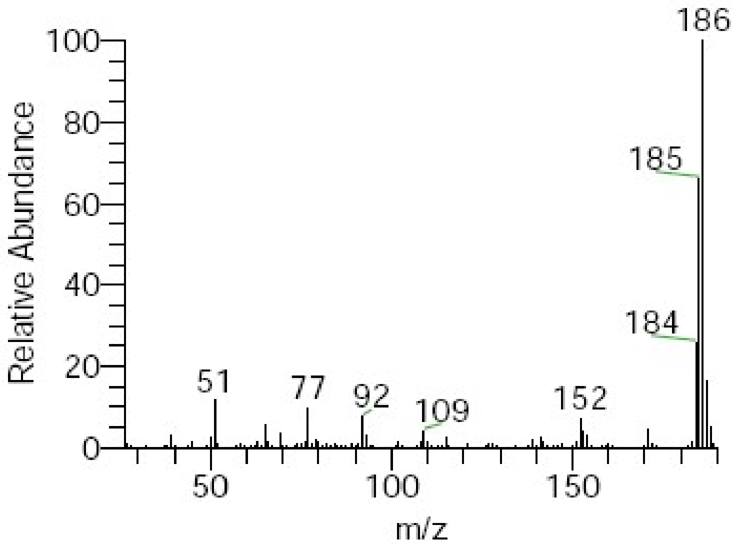

Figure S14. Mass Spectra of diphenylsulfane

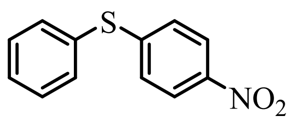

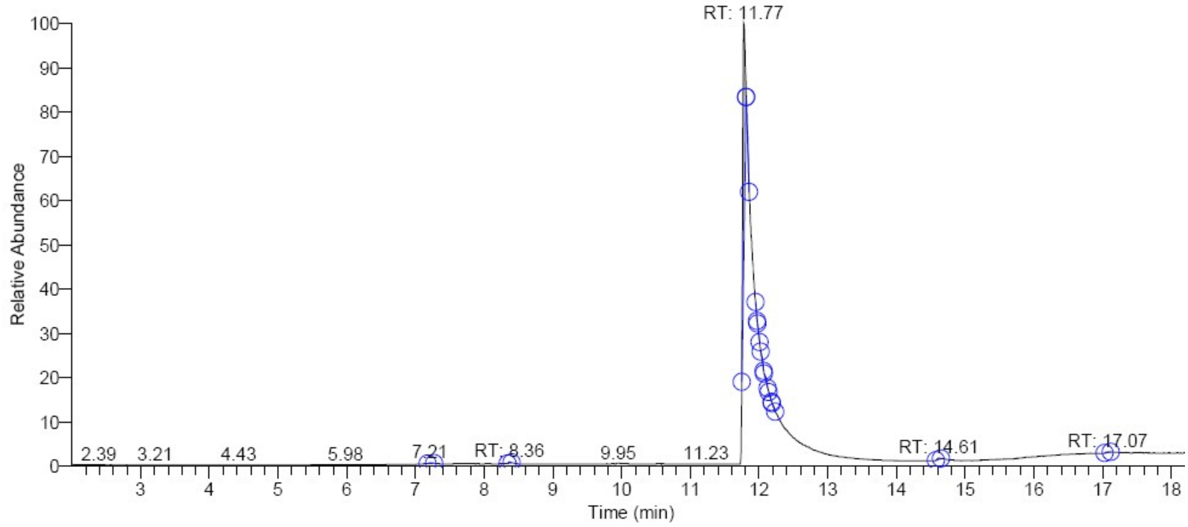

Figure S15.GC Spectra of (4-nitrophenyl)(phenyl)sulfane

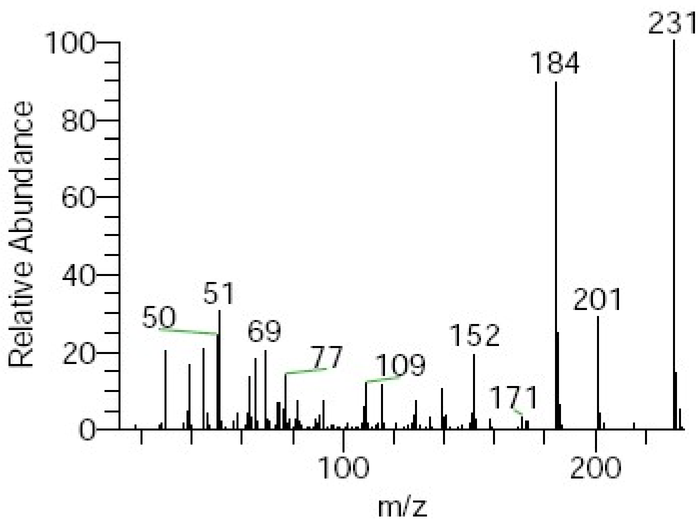

Figure S16. Mass Spectra of (4-nitrophenyl) (phenyl)sulfane

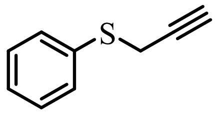

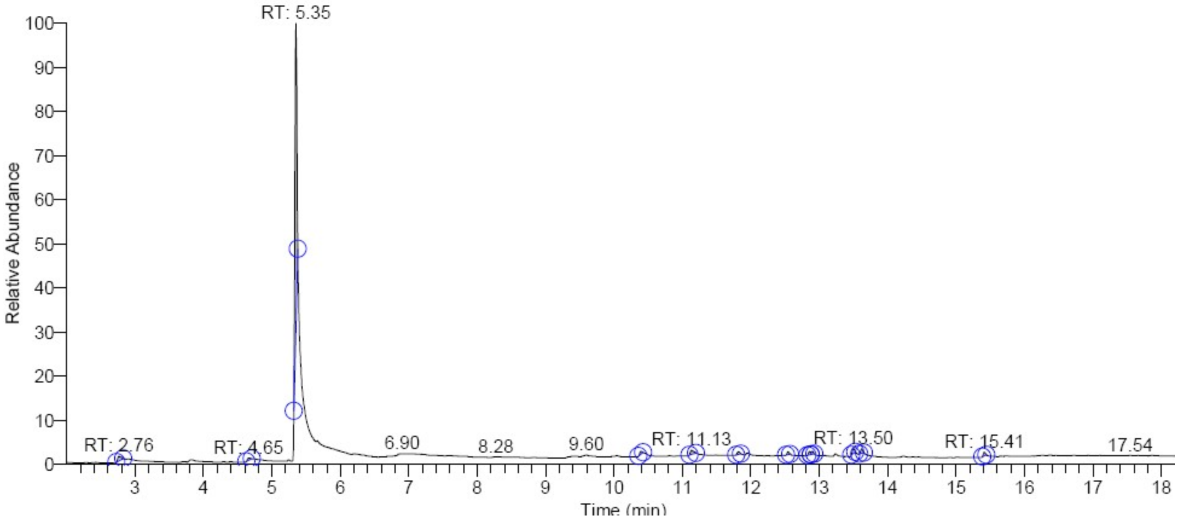

Figure S17.GC Spectra of phenyl(prop-2-yn-1-yl) sulfane

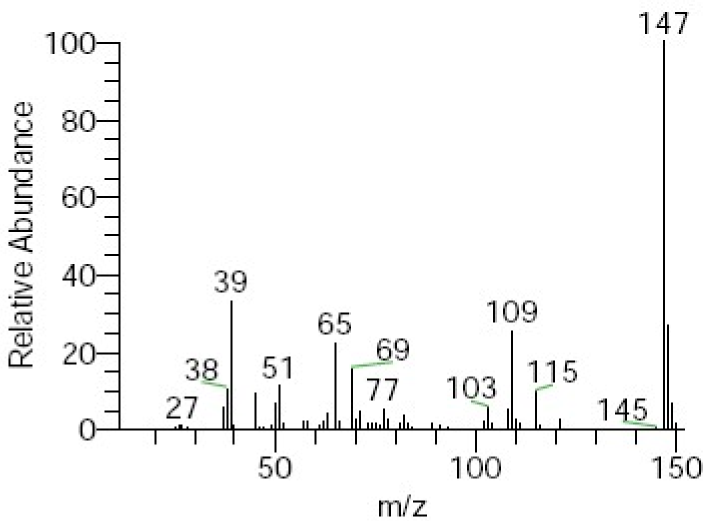

Figure S18. Mass Spectra of phenyl(prop-2-yn-1-yl) sulfane

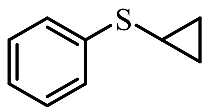

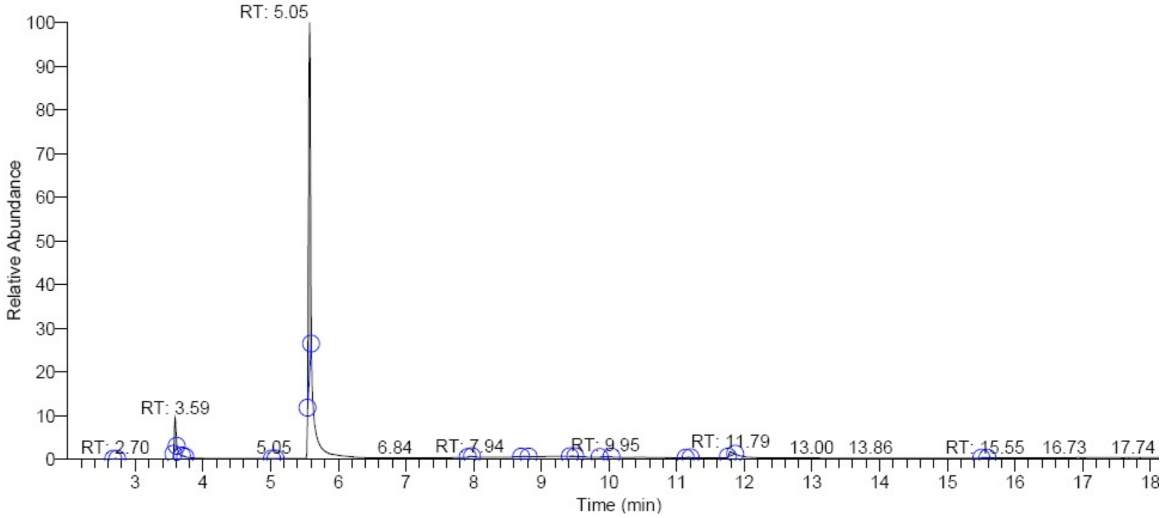

Figure S19.GC Spectra of cyclopropyl(phenyl)sulfane

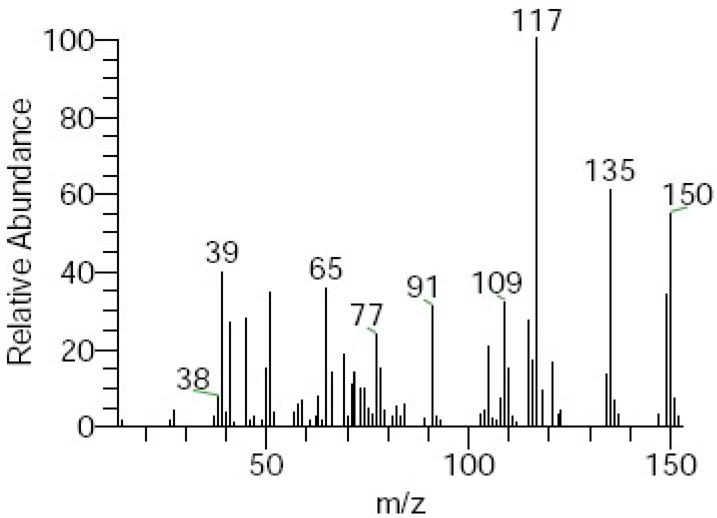

Figure S20. Mass Spectra of cyclopropyl(phenyl)sulfane

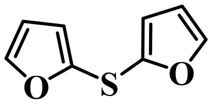

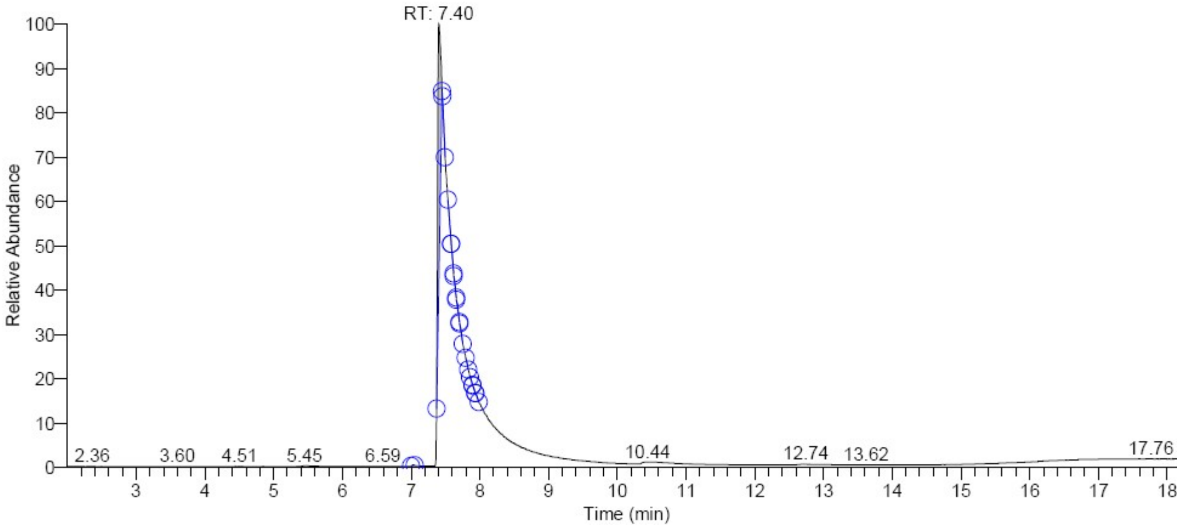

Figure S21.GC Spectra of di(furan-2-yl) sulfane

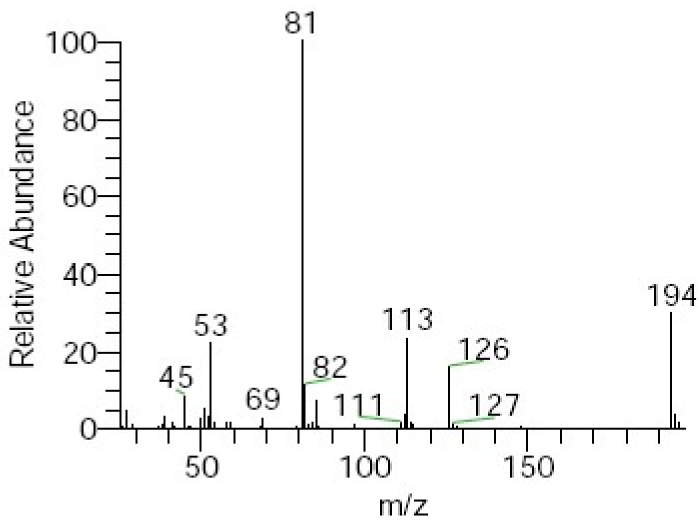

Figure S22. Mass Spectra of di(furan-2-yl) sulfane

References:

1. Ai, Q.; Yuan, Z.; Huang, R.; Yang, C.; Jiang, G.; Xiong, J.; Huang, Z.; Yuan, S., One-pot co-precipitation synthesis of Fe_3O_4 nanoparticles embedded in 3D carbonaceous matrix as anode for lithium ion batteries. *Journal of Materials Science* **2019,***54* (5), 4212-4224.